



Performance evaluation of a transmission tower by substructure test

Byoung-Wook Moon^a, Ji-Hun Park^b, Sung-Kyung Lee^a, Jinkoo Kim^c, Taejin Kim^c, Kyung-Won Min^{a,*}

^a Department of Architectural Engineering, Dankook University, Republic of Korea

^b Department of Architectural Engineering, University of Incheon, Republic of Korea

^c Department of Architectural Engineering, Sungkyunkwan University, Republic of Korea

ARTICLE INFO

Article history:

Received 30 July 2007

Accepted 12 April 2008

Keywords:

Transmission tower

Substructure test

Wind load

Buckling load

ABSTRACT

In this paper, a half-scaled substructure test was performed to evaluate the failure mode of an existing transmission tower subjected to wind load. A loading scheme was devised to reproduce the dead and wind loads acting on the prototype transmission tower. The load was enforced on the model structure using two actuators and a triangular jig mounted on the reduced model. Preliminary numerical analysis was carried out to evaluate the stability and member force of the specimen for the design load. When the substructured transmission tower was loaded by 270% of its maximum allowable buckling load, local buckling occurred in joints of leg members with weak constraints. From the experimental results, such as load–displacement curves, displacements, and strains of members, it was concluded that the local buckling was due to the additional eccentric force caused by unbalanced deformation of the specimen.

© 2008 Elsevier Ltd. All rights reserved.

1. Introduction

Recently, demand on electrical power has been increasing around the world and many large-scale transmission towers have been newly constructed. Many transmission towers located in an open terrain are exposed to strong winds. In 2003 nine transmission towers collapsed when the typhoon ‘Maemi’ swept the Korean peninsula causing enormous economical loss [10]. After the disaster, the Korean Electrical Power Corporation (KEPCO) revised the design code for transmission towers, reflecting the enhanced hazard level for wind load [5,6]. Guidelines for retrofit methods such as increasing member cross-sectional area or reducing unbraced length by installation of brace members were also proposed [5,6]. Many existing transmission towers in Korea have been retrofitted based on the enhanced design load and the recommended retrofit methods.

Albermani et al. [2] proposed retrofitting methods such as adding diaphragm and constraining the out-of-plane deformation of each face of transmission tower, and verified the performance both experimentally and numerically. Alam and Santhakumar [1] carried out a loading test of a 34 m-high transmission tower with a capacity of 220 kV, and found that the buckling of tower leg members and cross-arm bottom members caused failure of the transmission tower. Based on the test results, they suggested

the reduction of the maximum slenderness ratio, 150, regulated in the design codes [3,4] to 110. Momomura et al. [9] and Okamura et al. [11] investigated the dynamic characteristics of transmission towers built in mountainous areas based on wind-induced vibration data and numerical analysis. Kim and Lee [7] performed a loading test of a 78 m-high transmission tower constructed with circular tube sections.

In this paper, a half-scaled substructure test was performed to evaluate the behavior and failure mode of an existing transmission tower subjected to wind load. A loading scheme was devised to reproduce the gravity and wind loads acting on the prototype transmission tower. The load was enforced on the model structure using two actuators and a triangular jig mounted on the top of the specimen. Preliminary numerical analysis was carried out to evaluate the stability and member force of the specimen for the design load.

2. Test setup

2.1. Scaled model for a transmission tower

A 154 kV B2-type transmission tower of height 38.1 m illustrated in Fig. 1 was chosen as a prototype structure for experiment. In both sides of the tower 300 m-long electric wires are connected. For experiment two units in the middle of the tower were modeled with a 1/2 scale in length. In this case the cross-sectional areas are reduced to 1/4 of those of the prototype structure. The height of the test specimen is 3 m, and the plan dimensions of the bottom and top of the specimen are 2 m × 2 m and 1.5 m × 1.5 m, respectively.

* Corresponding address: Department of Architectural Engineering, Dankook University, San 44-1, Jukjeon-Dong, Suji-Gu, 448-547 Youngin-Si, Kyunggi-Do, Republic of Korea. Tel.: +82 31 8005 3734.

E-mail address: kwmin@dankook.ac.kr (K.-W. Min).

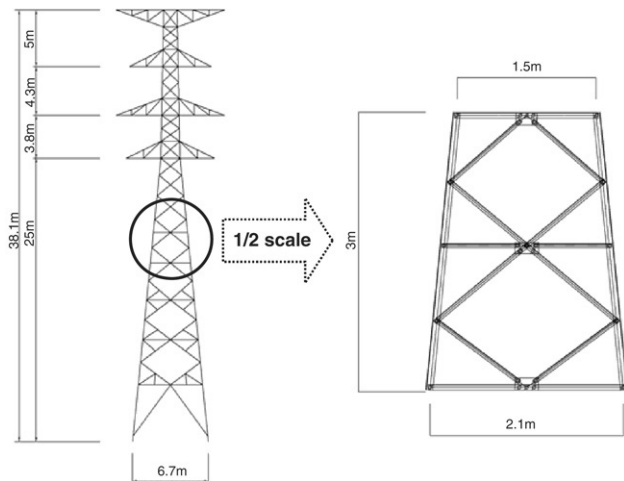


Fig. 1. A prototype transmission tower and a half scaled sub-assembly test model.

Table 1
Sectional properties of the prototype transmission tower

Section size (mm)	Cross-sectional area (cm ²)	Second moment of inertia (cm ⁴)	Radius of gyration (cm)
HL 150 × 12	34.77	304.00	2.96
L 65 × 6	7.537	12.20	1.27
L 60 × 4	4.64	6.62	1.19
L 50 × 4	3.84	3.76	0.983

Table 2
Sectional properties of the scaled model structure

Section size (mm)	Cross-sectional area (cm ²)	Second moment of inertia (cm ⁴)	Radius of gyration (cm)
L 75 × 6	8.727	19.00	1.48
L 60 × 4	4.692	6.62	1.19
L 45 × 4	3.492	2.69	0.88
L 45 × 4	3.492	2.69	0.88

The elements of the specimen are composed of angle sections made of SS400 steel ($F_y = 240$ MPa and $F_u = 330$ MPa). Member sizes and sectional properties of the prototype structure and the scaled test model are listed in Tables 1 and 2. Unlike the tower legs, the brace members have sections a little larger than the required ones due to the lack of the standard section satisfying the similarity law. However, since the forces in the bracing members are less than 4.5% of those of the tower legs, the inaccurate scale factors for the braces have little effect on the performance of a transmission tower. Zinc galvanized bolts with diameter of 16 mm (M16) were used instead of M20 for the same reason. To make the upper boundary conditions similar to the prototype structure, steel plates were welded to the top of the specimen and to the bottom of the jig.

2.2. Loading on the prototype and the test model structures

The loads acting on a transmission tower are as follows: vertical load; lateral longitudinal and transverse loads; and longitudinal unbalance load. The vertical load comes from mostly self-weight such as shield wires, conductors and insulators. The lateral longitudinal load is the tensile force of electric cables and shield wires. The lateral transverse load acts perpendicular to the direction of electric cables, and the wind load and the load due to angle of line deviation correspond to this category. The longitudinal unbalance load is the torsion caused by severance of transmission lines. The transmission towers are generally designed

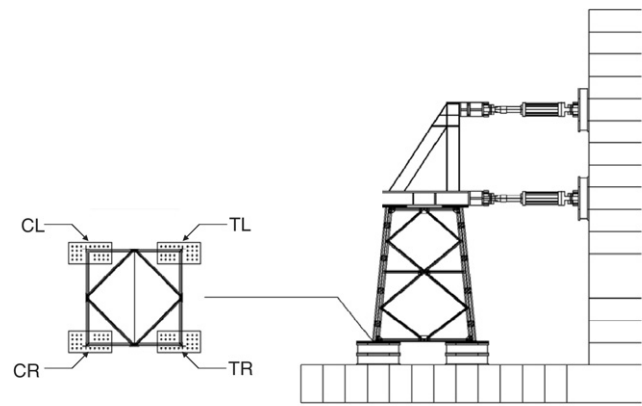


Fig. 2. Configuration of test model structure and actuators.

with maximum stress computed by various load combinations, including the loads described above. In this experimental study the load was enforced along the transverse direction considering the fact that the largest lateral load acts along that direction and that the experiment is carried out in a laboratory with limited number of actuators.

The load applied to the test specimen was determined following the similarity law. As the wind load is proportional to the surface area of the structure, the lateral load imposed on the test specimen is reduced to 1/4 of the design load of the prototype structure. As the weight is proportional to the volume of members, the dead load imposed on the model structure was reduced to 1/8. As the weight of the jig was similar to the dead load to be imposed on the test specimen, no additional load was applied.

Generally a loading test of full-scale transmission towers uses a wire connected to each loading point. But, in this study, two hydraulic actuators were used to apply desired loading on the specimen as shown in Fig. 2. The actuators impose both bending moment and lateral shear force to simulate the loads transmitted from the removed upper substructure through a triangular jig. This test setup has advantage in that local failure modes can be more thoroughly observed. The actuators with the capacity of 140 MN and 90 MN were placed at the height of 5 m and 3 m from the ground, respectively. The height of the specimen is 3 m, and the maximum height that an actuator can be placed in the laboratory is 5 m. Therefore a 2 m moment arm is available to impose bending moment on the specimen. However the moment arm required to meet the similarity law is approximately 8 m. To provide the specimen with equivalent bending moment the lateral force from the actuator should be increased significantly. This, however, results in unnecessarily high shear force acting on the structure. To reduce the shear force down to the design load level, another actuator was installed at the height of 3 m to apply load in the reverse direction. To carry out the experiment by displacement control, the displacement under design load was computed by numerical analysis, and the displacement was increased until failure of the structure. The test setup is depicted in Fig. 2.

2.3. Installation of strain gauges and LVDT's

The locations of strain gauges and the naming of elements and joints are shown in Fig. 3. The name of strain gauges located between the joints starts from M and the name of those placed near the joints starts from J. As the number of channels in the data logger is only 60 and there are many structural members, strain gauges were installed in limited locations. The expected failure mode of a transmission tower subjected to an overturning moment is the buckling of the compression members. According

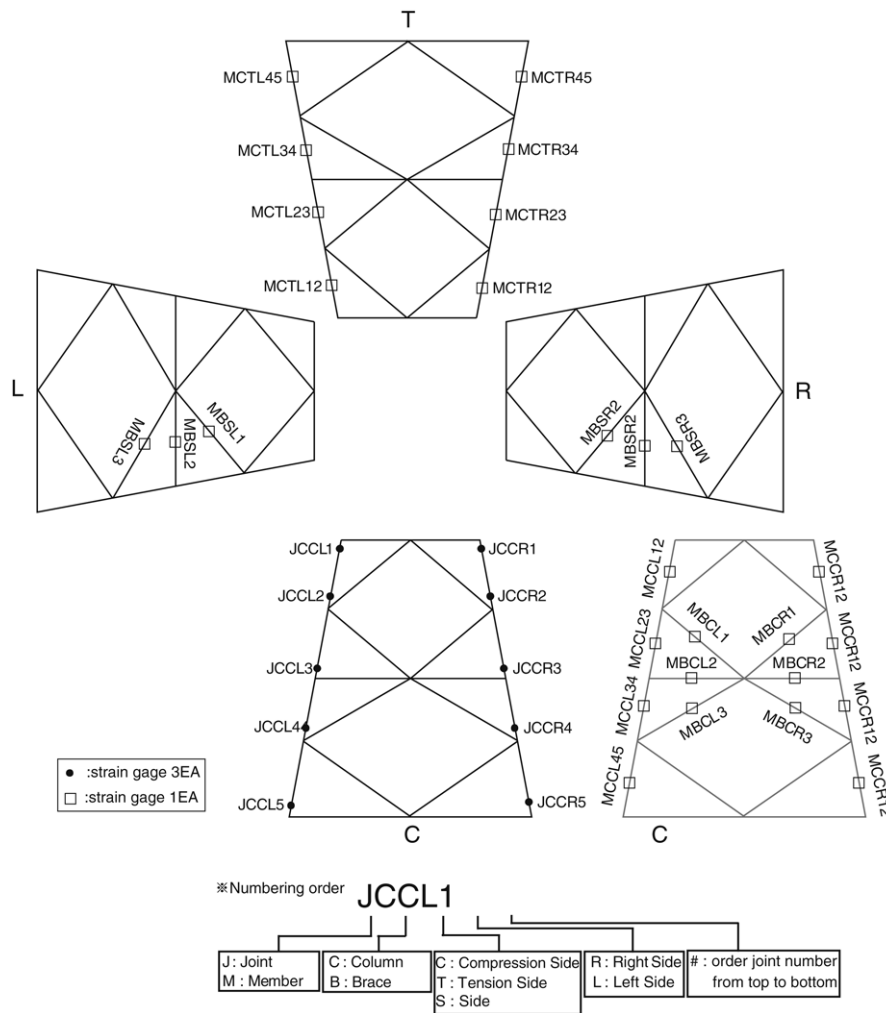


Fig. 3. Naming and location of strain gauges.

to the analysis results, the compression in bracing members is significantly smaller than the buckling load, and therefore most of the strain gauges were installed in leg members subjected to compression. As no axial force exists between the connections in columns subjected to compression, strain gauges were installed close to the connections. On the other hand, a strain gauge was placed between the connections in columns subjected to tension. In the tower lags subjected to compression, three strain gauges were installed at one place, at two ends and a corner of angle sections as shown in Fig. 4, to measure bending moment and axial force imposed on the section. On the other hand, in tower legs under tension the strain gauges were installed only in the middle of the upper legs, which were expected to experience the largest member force. In bracing members, the strain gauges were installed in the middle of the members. As the displacement at the top of the specimen along the loading direction is recorded by the actuator, two LVDT's were installed perpendicular to the loading direction. In the mid-height of the specimen under compression because no diaphragm action from the jig was expected (Fig. 5).

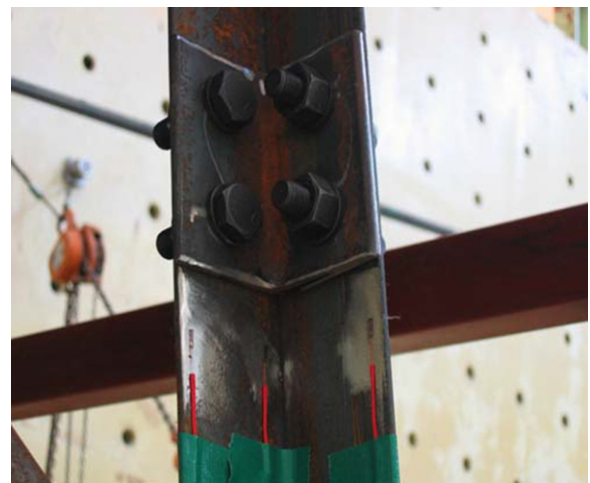


Fig. 4. Placement of strain gauges near a joint of a leg member.

3. Numerical analysis

3.1. Preliminary analysis

For numerical analysis the specimen was modeled by beam elements and all elements were assumed to be rigidly connected.

The triangular upper part of the jig was modeled by beam elements and the remaining lower part was modeled by shell elements. The beam and the shell elements were connected by rigid links. The numerical modeling and analysis of the model structure were carried out using the finite element analysis program package MIDAS-Civil [8]. Fig. 6 shows the analysis model of the test

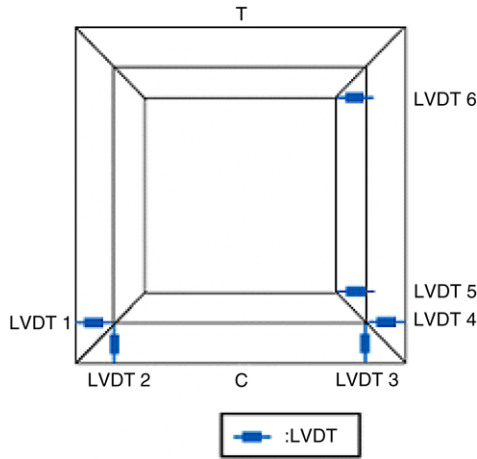


Fig. 5. Location of LVDT's.

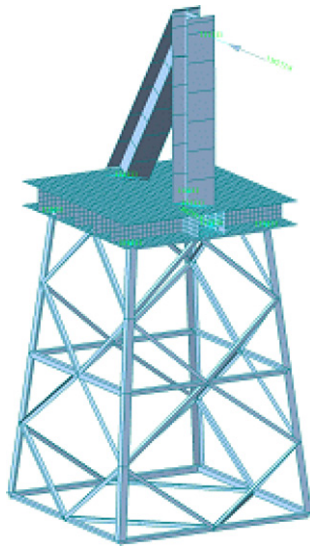


Fig. 6. Finite element modeling of the transmission tower test specimen (MIDAS Civil).

specimen. The applied load was obtained from the design load of the transmission tower (Tables 3–5).

The analysis results showed that the maximum displacement of the specimen was 3.217 mm with inter-story drift of 0.1072%. Even though the lateral displacement was not very large, significant amount of lateral drift was expected at the top of the prototype transmission tower considering the cantilever mode deformation of a transmission tower. Next the analysis results for member forces were compared with those computed by equations recommended by design guidelines for transmission towers [5,6]. The recommended equations are as follows:

- For structural members with small eccentricity (leg members, main members in cross arm)

$$t \leq 16 \quad \text{and} \quad 0 < \lambda_k < 105 : \sigma_{ka} = 1550 - 23(\lambda_k/100) - 602(\lambda_k/100)^2 \quad (1)$$

$$t \leq 16 \quad \text{and} \quad \lambda_k \geq 105 : \sigma_{ka} = 950(\lambda_k/100)^2. \quad (2)$$

- For structural members with small eccentricity (bracing members)

$$t \leq 16 \quad \text{and} \quad 0 < \lambda_k < 135 : \sigma_{ka} = 1550 - 762(\lambda_k/100) \quad (3)$$

$$t \leq 16 \quad \text{and} \quad \lambda_k \geq 135 : \sigma_{ka} = 950(\lambda_k/100)^2 \quad (4)$$

Table 3

Design load for prototype transmission tower perpendicular to the wind direction

Projected area of cross arms	1.41 (m ²)
Projected area of a tower body	9.29 (m ²)
Shear force by cross arms	4.78 (kN)
Shear force by a tower body	34.24 (kN)
Shear force by the load due to angle of line deviation	165.25 (kN)
Sum of upper shear force	198.84 (kN)
Sum of upper moment	2209.4 (kN m)

Table 4

Design gravity load on the prototype structure

Shield wire weight	14.58 (kN)
Conductor weight	85.5 (kN)
Upper tower weight	34.52 (kN)
Total weight	134.6 (kN)

Table 5

Loads imposed on the test specimen

Upper actuator force	137.2 (kN)
Lower actuator force	–88.2 (kN)
Gravity load	16.86 (kN)

where λ_k is the effective slenderness ratio of a member, l_e/γ , where l_e is the effective length and γ is the radius of gyration of a member. In transmission towers the following values are generally used for effective length: for leg members, $l_e = 0.9l$; for bracing members, $l_e = 0.8l$. The member forces of the compression members obtained from numerical analysis and the buckling strengths obtained from Eqs. (1) to (4) are presented in Table 6, where the values inside of the parentheses are the ratios of the buckling strengths obtained from numerical analysis and from the formulas. It can be observed in Table 6 that the axial forces of leg members computed by numerical analysis ranged from 80% to 90% of the allowable buckling loads. Therefore the test specimen was considered to have enough strength for the design load. When the structure is subjected to external load greater than the design load the leg members at the lower part of the specimen are most vulnerable for buckling. On the other hand, the member forces in the bracing members were less than 13% of the allowable buckling strength. This is due to the fact that the structure is mainly deformed in bending mode, and therefore it can be expected that the reinforcement of the braces will not increase the strength and stiffness of the transmission tower significantly. This observation may justify the use of braces with slightly larger cross-sectional areas than required by the similarity law in this experimental study.

3.2. Nonlinear analysis

Nonlinear analysis of the specimen was carried out using the finite element analysis program ANSYS Structural Utility. Nonlinear material property was found from the coupon test result shown in Fig. 7. Fig. 8 shows the nonlinear analysis model of the test specimen. The triangular upper part of the jig and angle members were modeled by BEAM 188. The plate steel part of the jig was considered as a rigid link since it shows rigid body motion during the experiment. The bolt connection was modeled by COMBIN7 to consider applied torque of the bolt. COMBIN7 is a 3-D pin joint which may be used to connect two or more parts of the model at a common point. Capabilities of this element include joint flexibility (or stiffness), friction, damping, and certain control features. An important feature of this element is a large deflection capability in which a local coordinate system is fixed to and moves with the joint. Fig. 9 shows the stress distribution and deformation shape of a test specimen as a result of the nonlinear analysis.

Table 6
Member forces and allowable buckling loads of compression members

Members	Length (cm)	Slenderness ratio	Allowable buckling stress ($\times 10^4$ kPa)	Allowable buckling load (kN)	Preliminary analysis results (kN)
MCCL12 MCCR12	72.7	28.4	-14.64	-127.38	-101.71 (79.9)
MCCL23 MCCR23	69.4	27.2	-14.69	-127.8	-106.38 (83.2)
MCCL34 MCCR34	81.9	32.0	-1.480	-126.18	-106.19 (84.2)
MCCL45 MCCR45	72.7	28.4	-14.50	-127.38	-112.11 (88.0)
MBSL1 MBSR1	107.7	71.8	-9.82	-34.37	3.2 (-9.3)
MBCL1 MBCR1					-1.86 (5.4)
MBSL2 MBSR2	79.50	53.0	-11.23	-39.31	0.85 (-2.2)
MBCL2 MBCR2					1.57 (-3.9)
MBSL3 MBSR3	118.1	78.7	-9.31	-32.59	-4.29 (13.2)
MBCL3 MBCR3					-2.18 (6.7)

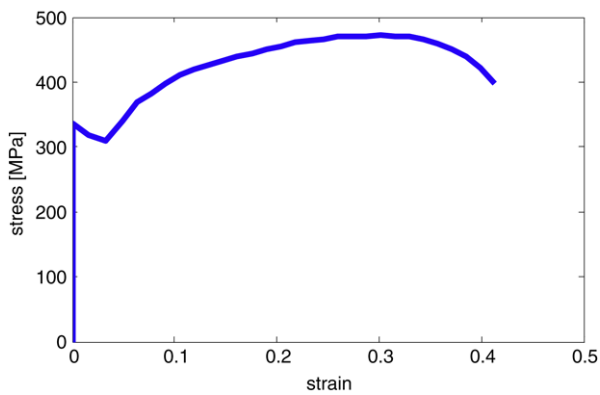


Fig. 7. Stress-strain curve of the steel angle (coupon test result).

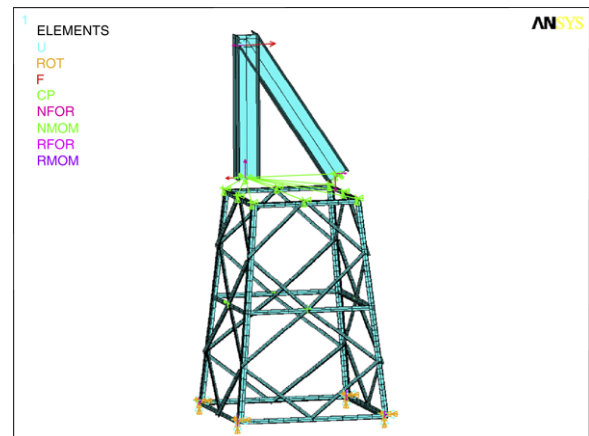


Fig. 8. The nonlinear analysis model of the transmission tower test specimen (ANSYS Structural U).

Table 7
Strains of bracing members obtained by preliminary analysis and experiment

Members	Experiment (10^{-6})	Nonlinear analysis (10^{-6})	Experiment/analysis
MBSL1	28.56	20.16	1.42
MBSR1	77.11	62.34	1.24
MBCL1	-19.04	-15.95	1.19
MBCR1	4.76	5.03	0.95
MBSL2	-2.86	-2.97	0.96
MBSR2	-10.47	7.27	-1.44
MBCL2	8.57	6.59	1.30
MBCR2	15.23	6.59	2.31
MBSL3	-28.56	-34.73	0.82
MBSR3	-27.61	-32.52	0.85
MBCL3	13.32	-6.49	-2.05
MBCR3	-24.75	-16.70	1.48

It is observed that the yield stress occurred in the “JCCL2” and “JCCR3”. This local buckling in both “JCCL2” and “JCCR3” coincides with the experimental results shown in Fig. 10. Accordingly, the nonlinear analysis results performed in this study can estimate the experimental results.

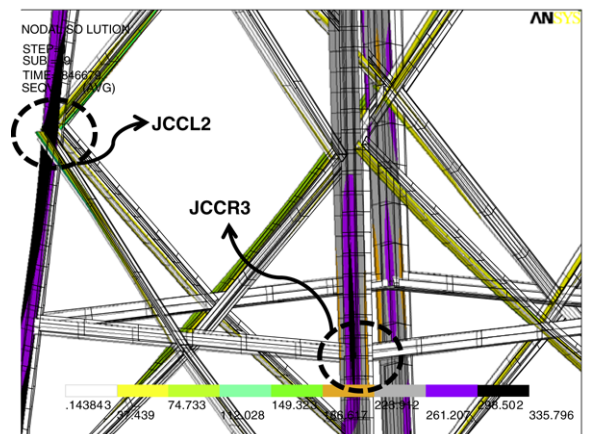


Fig. 9. Von Mises stress and deformation of nonlinear analysis results.

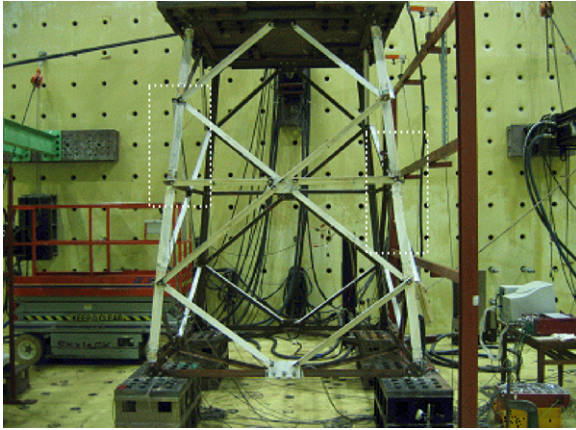


Fig. 10. Photograph of the specimen after loading is over.

Table 8
Top displacement when yield strains of the leg members are reached (mm)

Location	JCLL			JCCR			MCTL	MCTR
	Left	Corner	Right	Left	Corner	Right		
1	6.721	12.77	9.990	18.44	14.70	6.864	12.02	10.27
2	16.66	10.69	9.514	9.608	11.55	14.61	10.04	10.18
3	10.27	8.521	10.93	10.31	8.569	15.26	10.31	10.65
4	9.423	11.45	9.514	18.13	10.37	16.70	9.085	11.22
5	18.44	9.276	6.155	7.528	9.185	11.78	.	.

4. Test results

4.1. Deformed configuration

The load was imposed on the specimen gradually by displacement control. In the initial stage of the experiment no discernible change in configuration was observed. At the actuator displacement of 37 mm local buckling occurred at one of the columns. After this point the applied load rapidly decreased and the application of load was stopped when the applied load reduced to about 70% of the maximum load. The relative displacement of 0.01 mm was observed between the top and the bottom of the jig, which can be neglected.

Fig. 10 shows the side view of the specimen after loading was over. It can be observed that global buckling did not occur in any member under compression. However it can be noticed in Fig. 11 that the column was twisted due to local buckling. The parts in which local buckling occurred are shown in Fig. 10 enclosed in the dotted rectangles. The joint of the column which experienced local buckling and is shown in the right-hand-side of Fig. 10 is depicted in Fig. 11.

The parts of leg members located in the top and bottom of the specimen, MCCR12 and MCCR45, respectively, did not undergo discernable deformation. However the parts located in the mid-height of the specimen, MCCR23 and MCCR34, experienced large deformation as a result of local buckling at the joint JCCR3. The global buckling seemed to be prevented by the bracing members. At the joint JCCR3 the two connected members MCCR23 and MCCR34 were twisted in opposite directions. The reason for the occurrence of the largest torsional deformation at JCCR3 is that at that joint only one bracing member was connected to each channel-shaped leg member, while two bracing members were connected to a leg member at the joints JCCR2 or JCCR4 providing stronger support for movement of the leg members. As was observed in the preliminary analysis results, the horizontal bracing

member did not participate significantly in resisting lateral load, which implies that their contribution as lateral supports is minute.

Deformation of bracing members was observed only in members connected to the joints with large torsional deformation, JCCR3. As the bracing members are relatively slender compared with the leg members, the inelastic deformation caused by torsion was not significant.

In summary, the collapse of the transmission tower started from the local buckling of leg members near the joint with weaker lateral support. Therefore, for more effective reinforcement of a transmission tower, the strength for local and global buckling of leg members near the joints with weaker lateral support needs to be increased.

4.2. Load–displacement relationship

It was observed from the load–displacement curves that the lateral displacement obtained from experiment was similar to the displacement computed from nonlinear analysis. Fig. 12 shows the load–displacement curves recorded by the two actuators.

The yield or fracture of members can be noticed by the decrease of stiffness in the load–displacement curves. It can be observed that the slopes of the curves decrease gradually as the displacement of the lower actuator exceeds about 6 mm. Considering that the decrease of stiffness occurred before member yield strain was reached, this may have been caused by the slip in bolted connections.

Fig. 13 presents the slopes of the load–displacement curves recorded by the actuators. It can be observed that rapid change in slope occurred when the displacement of the lower actuator reached 13.5 mm, 15.2 mm, and 16 mm. The change in slope was accompanied by drastic reduction and subsequent recovery followed by a gradual decrease in slope. This phenomenon is considered to be associated with the buckling of a member and following redistribution of member forces. As will be stated later, the points of stiffness reduction match well with those of rapid change in strain and member forces. It also can be observed that stiffness decreased minutely before abrupt change in stiffness, which becomes noticeable after the actuator displacement exceeds 26 mm and 11 mm. This is considered to have been caused by yielding of members rather than bolt slip.

4.3. Displacement

Fig. 14 shows the horizontal displacement of the specimen perpendicular to the loading direction, where the horizontal axis represents the corresponding displacement in the loading direction. The large difference in the data recorded in the two LVDT's mounted on the upper part of the specimen implies that the specimen was twisted during the experiment. The difference in displacement was transformed to the twisting angle and is presented in Fig. 15. As the lateral displacement along the loading direction exceeds 10 mm, the rate of change in twisting angle increases, which corresponds to the point where the slope of the load–displacement curve shown in Fig. 13 decreases significantly. Also, the twisting angles suddenly changed when the displacement in the loading direction reached 15.1 mm, which corresponds with the point that actuator load dropped rapidly as shown in Fig. 13. The maximum rotation, however, turned out to be approximately 0.11° and the effect of torsion is not considered to be significant. It can be seen in Fig. 14(a) that the displacement measured by the LVDT1 located at the lower part of the leg member MCCL23, which experienced local buckling, changed significantly when the top displacement along the loading direction reached 13.5 mm. Therefore it can be concluded that the abrupt change in stiffness

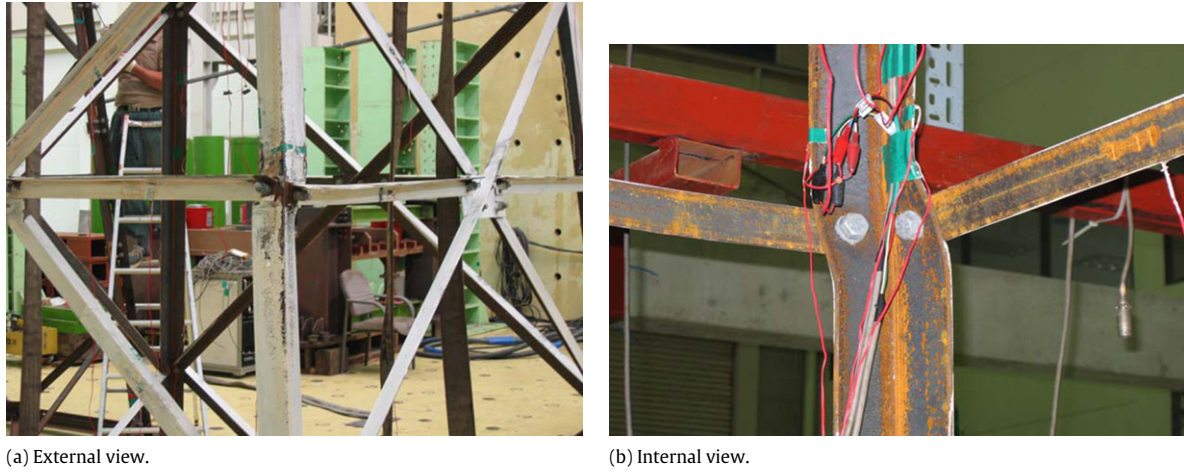


Fig. 11. Deformation of the leg member near the joint JCCR3.

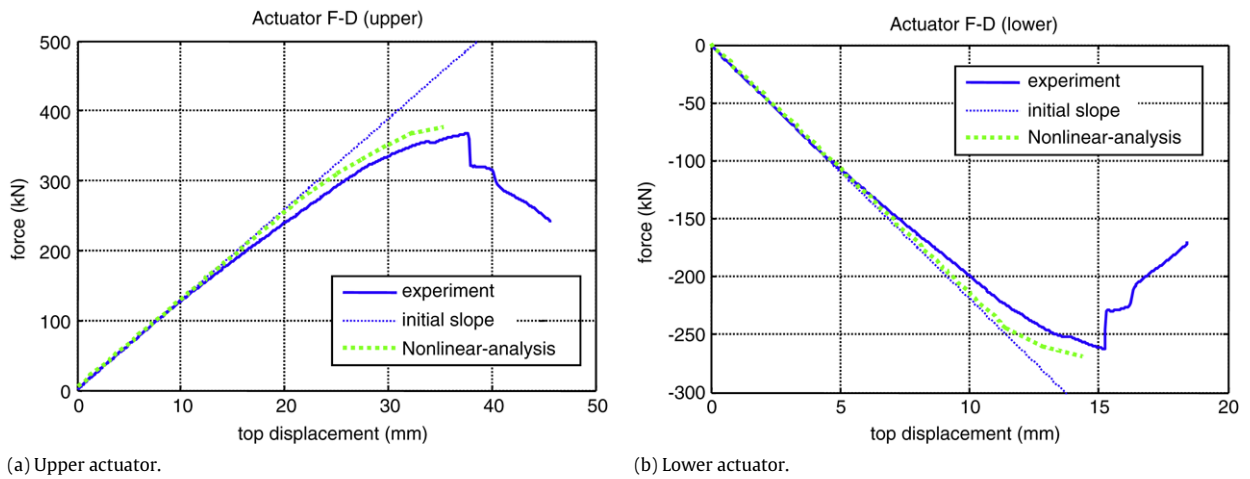


Fig. 12. Load–displacement curves of the test specimen at the location of actuators.

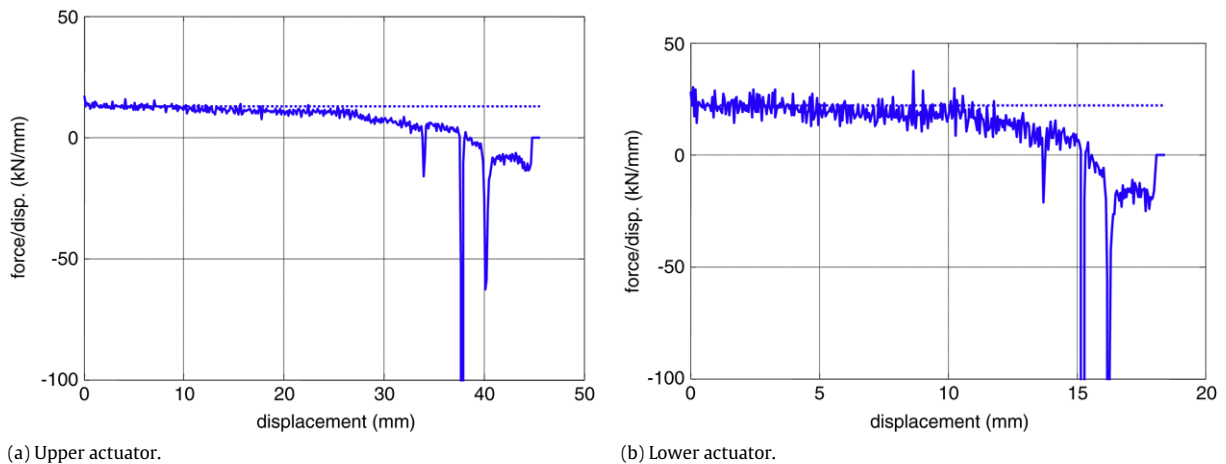


Fig. 13. Slope of the load–displacement curves of the test specimen measured by actuators.

observed in the load–displacement curves shown in Fig. 12 was caused by local buckling of the leg members MCCL23. On the other hand, the displacement measured by LVDT4 located at the lower part of the leg member MCCR23 increased rapidly when the displacement at the loading direction reached 15.1 mm. This indicates that the second rapid change in stiffness shown in Fig. 12 was due to the local buckling of the leg member MCCR23.

4.4. Strain of members

Fig. 16 shows the strain of the left-hand-side leg members subjected to compression. As shown in Fig. 4 three strain gauges, named as ‘left’, ‘corner’, and ‘right’ viewed, were installed at one place. At joints JCCL1, JCCL2, and JCCL3 the strains recorded by the three strain gauges increased linearly until the top

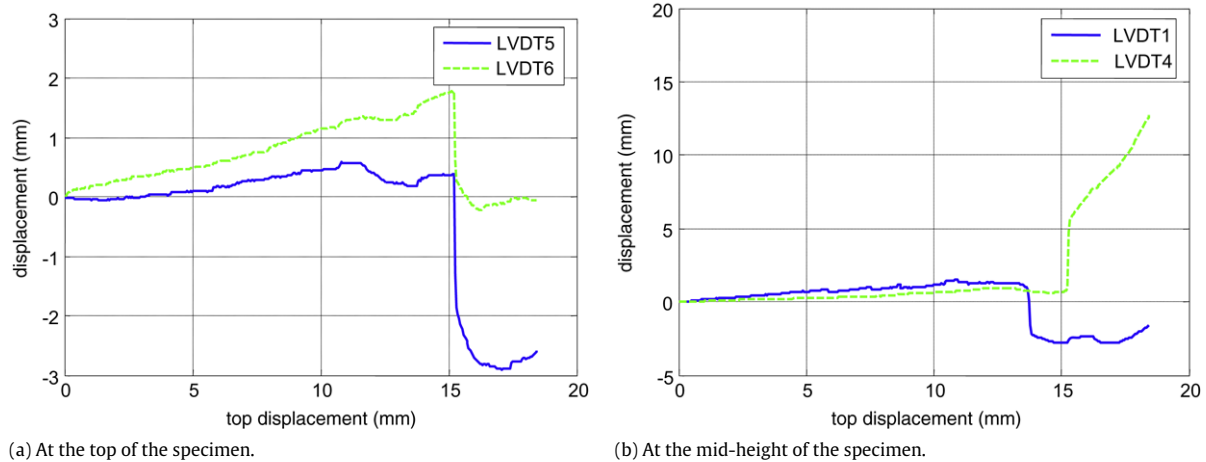


Fig. 14. Lateral displacements perpendicular to the loading direction.

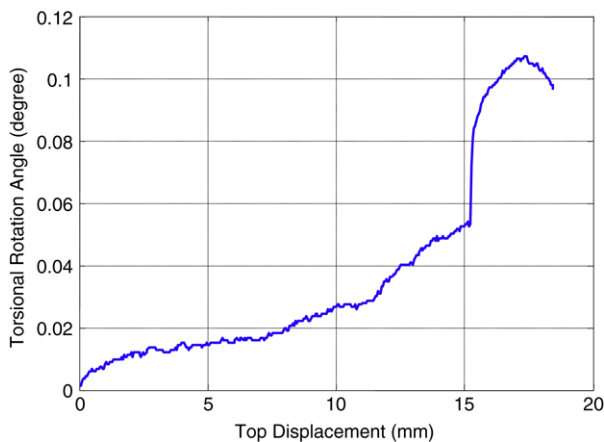


Fig. 15. Torsional rotation angle at the top of the specimen.

displacement reached 10 mm. Then local buckling occurred and the strains became highly nonlinear. At joints JCCL4 and JCCL5 such phenomenon occurred in the earlier stage, at around the top displacement of 5 mm. This is considered to have been caused by bolt slip or local yielding around the bolt holes. Based on the load–displacement curves it was observed that at the top displacement of about 13.5 mm the first local buckling occurred at the left-hand-side leg member subjected to compression. However, at this moment the strains did not change significantly, probably because the distance between the location of the strain gauges and the point of local buckling was far enough. After the top displacement exceeded 15.1 mm, local buckling occurred at the right-hand-side leg member, which caused a large bending moment at the left-hand-side joints (JCCL11, JCCL12) and significant change in strains.

Fig. 17 shows the strains measured at the right-hand-side leg members subjected to compression. As was observed in the left-hand-side leg members, the strains increased linearly. However after the top displacement exceeded about 7 mm and local buckling occurred at the joints, the measured strains changed rapidly. It also can be observed that at joints JCCR3 and JCCR4, in which local buckling occurred, significant amount of strains were measured. However at joints JCCR1, JCCR2, and JCCR5, the measured strains did not increase further because the load carrying capability of the member MCCR34 decreased after local buckling. The compressive strains measured by the 'left' and 'corner' gauges placed near the joint JCCR3 increased significantly due to the yielding of material, whereas in the 'right' gauge the compressive

strain changed to tensile strain due to bending deformation. On the other hand at joint JCCR4 the compressive strain of 'right' gauge increased rapidly and those of the 'left' and 'corner' gauges decreased significantly or even were reversed to tensile strains, which implies that bending and torsional deformation occurred. According to the displacement of the specimen in the transverse direction shown in Fig. 14(b), the first local buckling occurred at the left leg members. However before the local buckling occurred, when the top displacement reached approximately 12 mm, the strain in the 'corner' gauge at JCCR3 showed rapid increase. This seems to have been caused by yielding of the member considering the fact that no rapid variation was observed in the displacement recorded by LVDT4 placed in the middle of the right leg member.

Fig. 18 shows the strains of the leg members subjected to tension. Even though the strains far exceeded the yield strain of SS400 steel, 0.001190, the members were considered to have remained elastic as no abrupt changes were observed in the measured strain data. Fig. 18(a) shows that the strains obtained from the 'left' and 'right' strain gauges attached to the left leg members were similar to each other. On the other hand rates of increase in the strains obtained from both ends of the right leg members were reversed after the top displacement exceeded 9 mm as can be seen in Fig. 18(b). This showed that bolt slip occurred at the right leg members.

Fig. 19 depicts the strains of the bracing members, and the strains obtained from experiment and nonlinear analyses were compared in Table 7. It can be observed, especially in the bracing member MBSL1, that as a result of bolt slip the strains did not increase linearly. The difference between the strains obtained from experiment and analysis is also considered to be originated from bolt slip. It also can be noticed that right after the first and the second local buckling in members and subsequent redistribution of member forces, the strains of bracing members changed significantly.

Table 8 shows the top displacement along the loading direction when yield strain was reached. Smaller displacement at yield implies that the point yielded at an earlier loading stage. The strains of bracing members were not included because they were much smaller than yield strain. It can be observed that the top of the leg members subjected to compression yielded first. This is due to the fact that as the top of the specimen was welded to the plates on which the jig was mounted, stress was concentrated around the welded parts. However due to the stiffening effect of the jig, local buckling was prevented in this region. The middle of the leg members yielded at the top displacement of 9 mm, which was before the first local buckling occurred. Therefore the yield of the mid-part of the leg members resulted from the additional

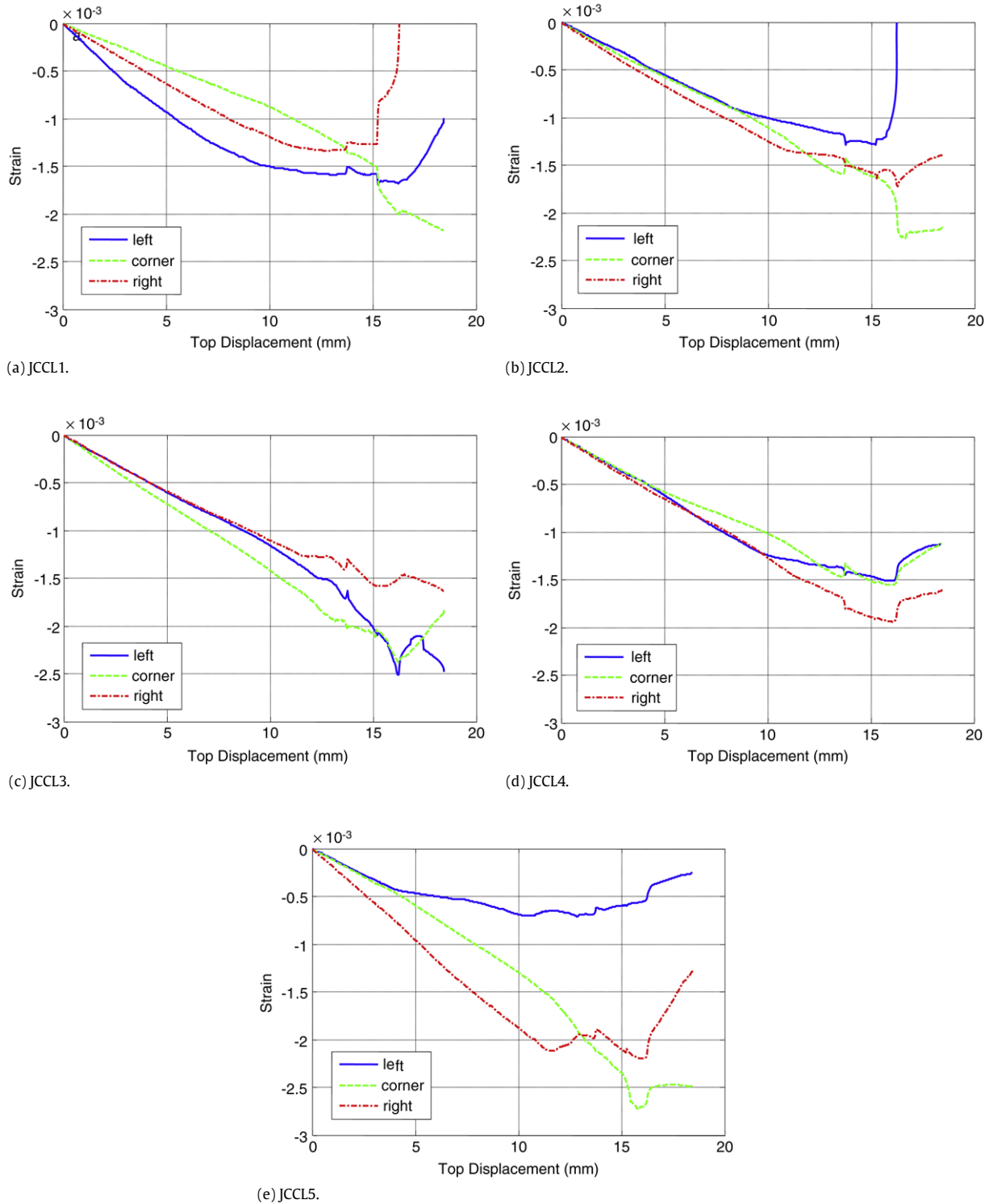


Fig. 16. Strain of the left leg member subjected to compression.

deformation due to torsion. Based on these observations, it can be concluded that to increase lateral strength of a transmission tower it would be necessary to prevent unbalance deformation and local buckling by increasing member size or adding stiffeners.

5. Conclusions

Sub-assembly test of a half-scaled transmission tower was carried out to estimate its performance against wind load. A

loading scheme was devised to reproduce the gravity and wind loads acting on the prototype transmission tower.

The axial forces of leg members subjected to design load computed by numerical analysis corresponded to 80%–90% of the allowable buckling loads. On the other hand, the axial forces of bracing members turned out to be less than 13% of the buckling loads, which implies that adding additional braces may not increase stiffness and/or the strength of a transmission tower significantly.

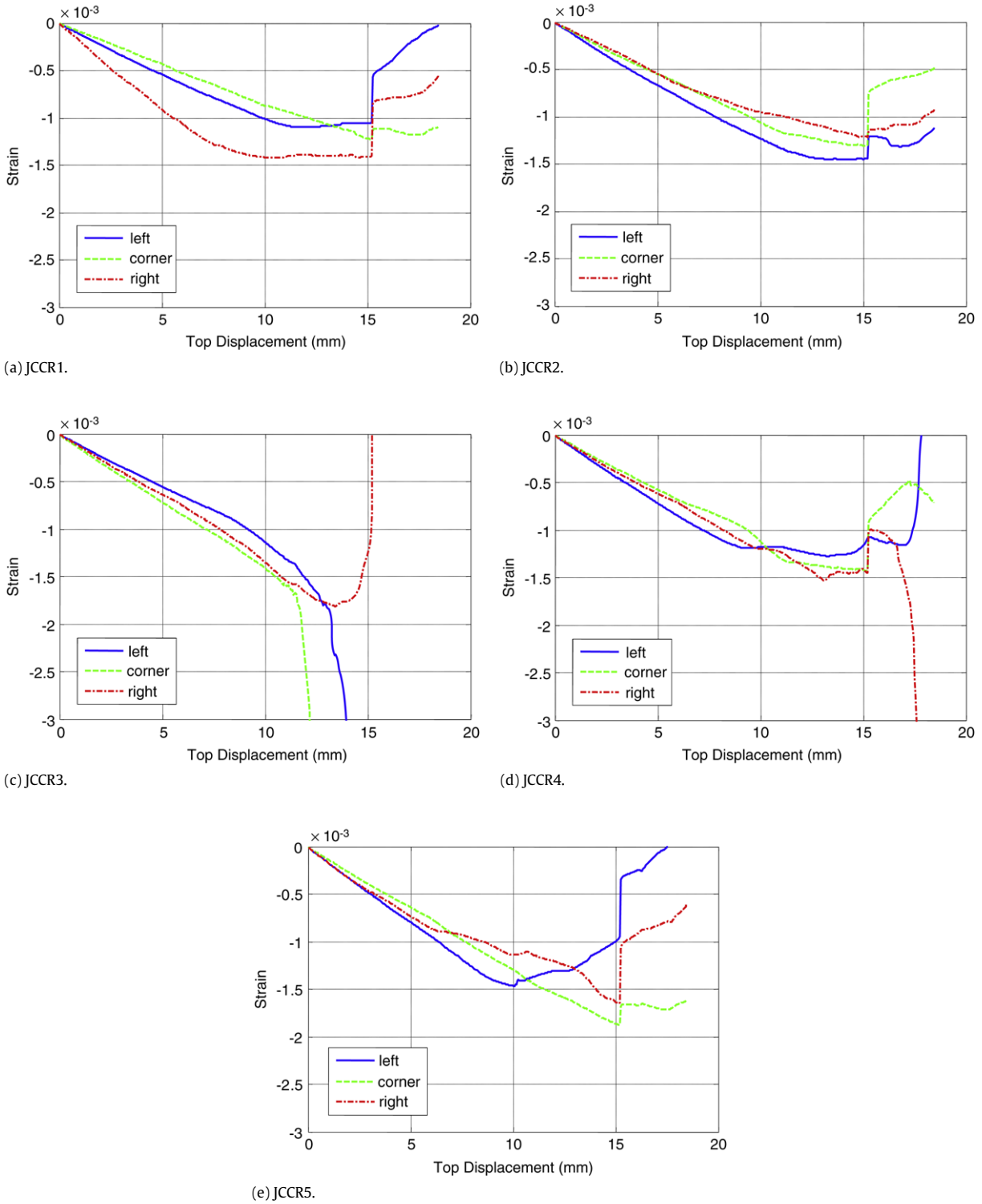


Fig. 17. Strain at joints of the right leg member subjected to compression.

From the experiment it was observed that local buckling occurred at the two leg members subjected to compression. According to the load–displacement curves and the strain data, the local buckling occurred as a result of the bending moment caused by unbalanced deformation as well as axial compression. To prevent unbalanced deformation and associated local buckling it would be necessary to increase member size or to add stiffeners on weak joints.

Acknowledgements

This work was partly supported by the Ministry of Construction & Transportation of Korea (C105A1050001-05A0505-00210) and by the Korea Science & Engineering Foundation (Grant No. R11-2002-101-03004-0 and R0A-2006-000-10234-0). Their financial supports are gratefully acknowledged.

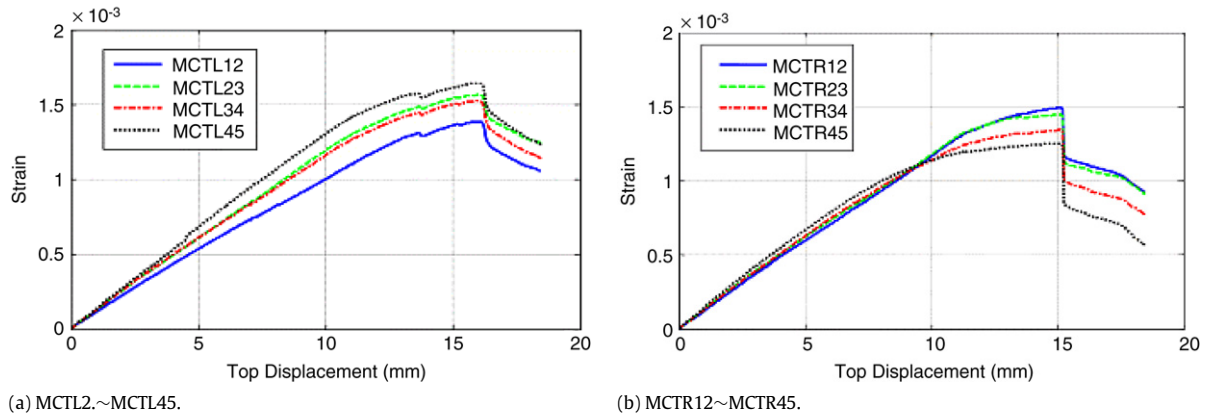


Fig. 18. Strain at various locations in members subjected to tension.

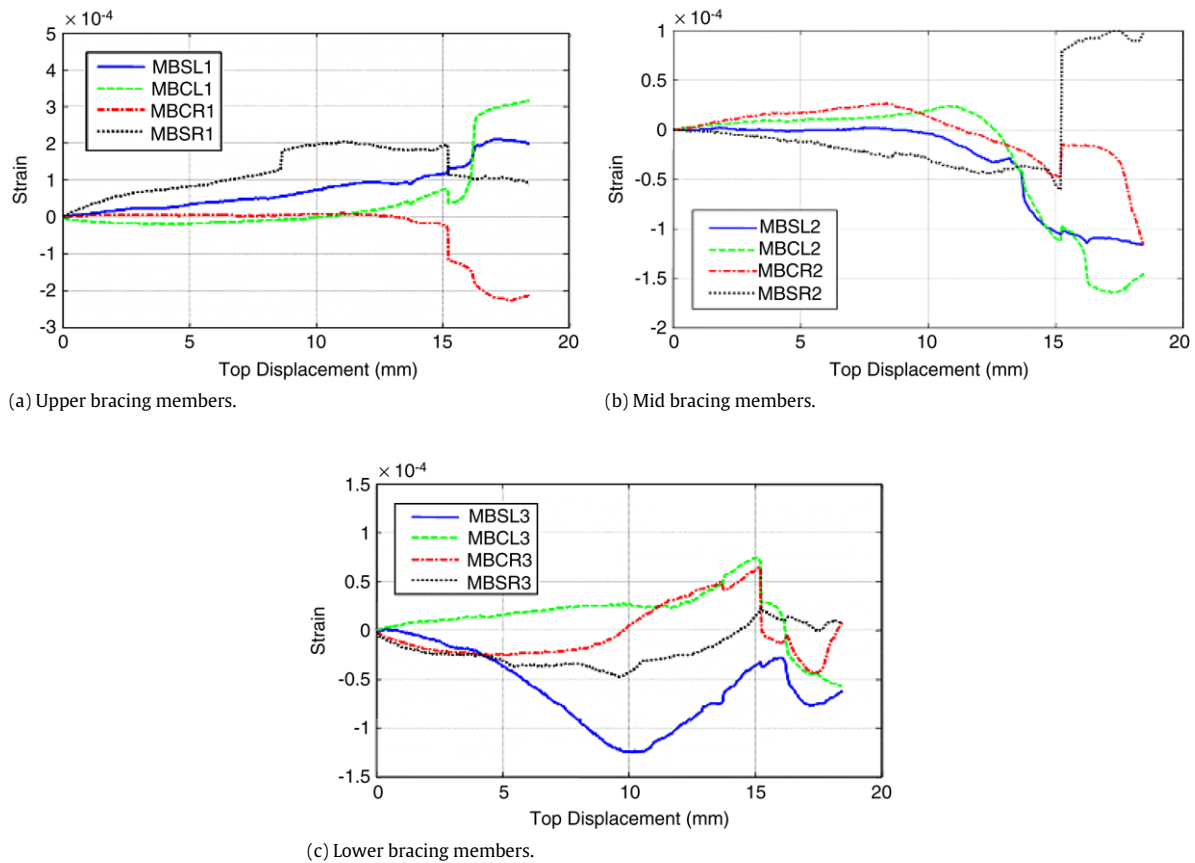


Fig. 19. Strain of bracing members.

References

- [1] Alam MJ, Santhakumar AR. Reliability analysis and full-scale testing of transmission tower. *Journal of Structural Engineering*, ASCE 1996;122(3): 338–44.
- [2] Albermani F, Marhendran M, Kitipornchai S. Upgrading of transmission towers using a diaphragm brace system. *Engineering Structures* 2004;26: 753–754.
- [3] ASCE manuals and reports on engineering practice No. 52; guide for design of steel transmission towers. 2nd ed. New York (NY): ASCE; 1988.
- [4] Indian standard code of practice for use of structural steel in overhead transmission line towers. New Delhi (India): IS:802, Bureau of Indian Standards; 1992.
- [5] KEPCO. Design standard for transmission towers. Korean Electrical Power Corporation; 2004.
- [6] KEPCO. Evaluation of the retrofitting methods for transmission tower body. Korean Electrical Power Corporation; 2004.
- [7] Kim WB, Lee KJ. Loading test of a full-scale transmission tower. Technical article. Korea Institute of Steel Structures; 1998.
- [8] MIDASIT. MIDAS gen analysis & design manual. MIDAS Information Technology Cooperation; 2004.
- [9] Momomura Y, Marukawa H, Okamura T, Hongo E, Ohkuma T. Full-scale measurements of wind-induced vibration of a transmission line system in a mountainous area. *Journal of Wind Engineering and Industrial Aerodynamics* 1997;72:241–52.
- [10] NIDP. Report on the damage caused by typhoon Maemi. Seoul (Korea): National Institute for Disaster Prevention; 2003.
- [11] Okamura T, Ohkuma T, Hongo E, Okada H. Wind response analysis of a transmission tower in a mountainous area. *Journal of Wind Engineering and Industrial Aerodynamics* 2003;91:241–52.